# Visualizing the inner workings of L-CNNs

**Andreas Ipp**

Institute for Theoretical Physics, TU Wien, Austria

June 27, 2023

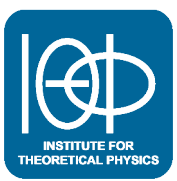




# QCD phase diagram

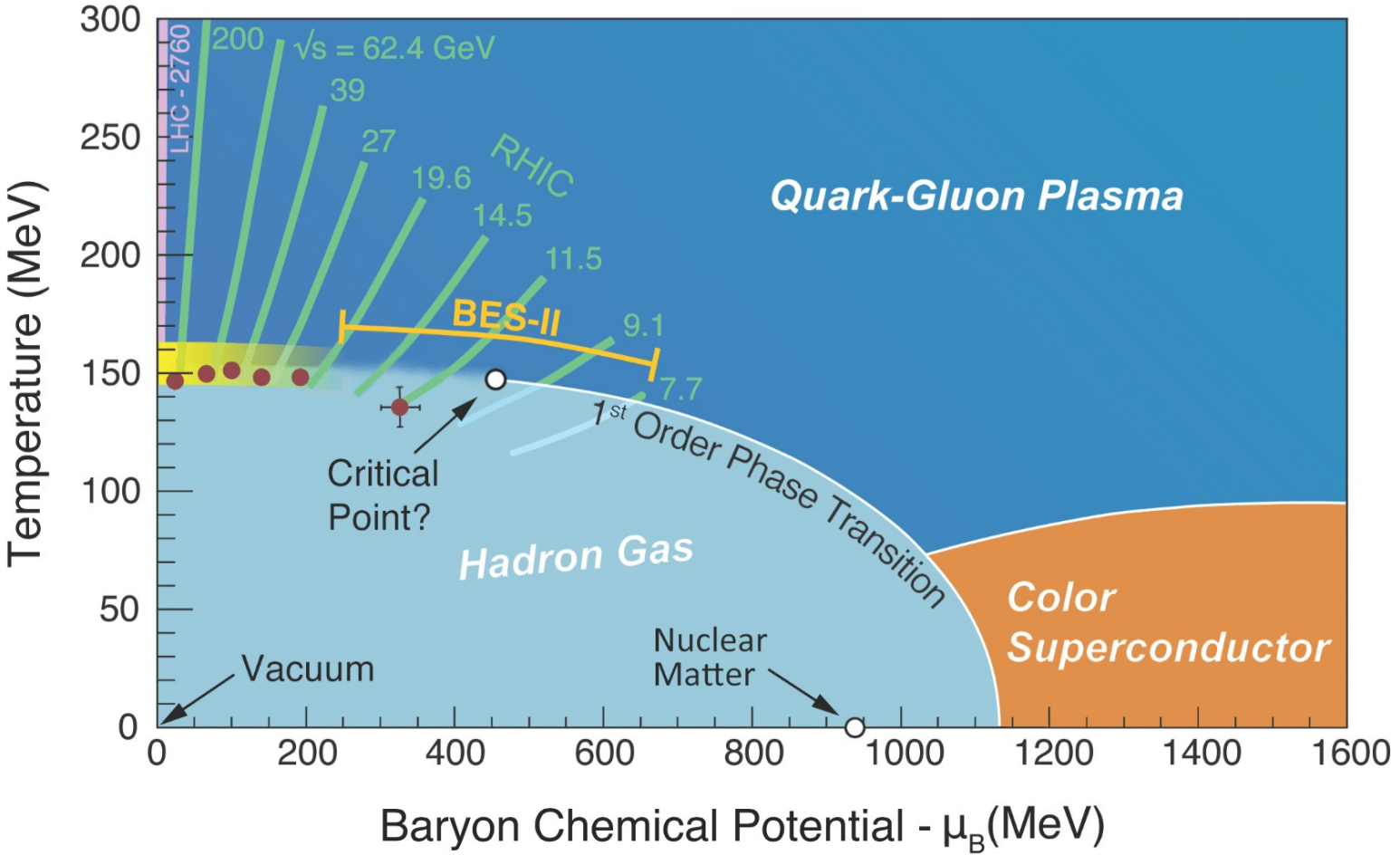


Sun (surface):
6000°C ≈ 0.5 eV

Sun (core):
15 million °C ≈ 1.3 keV

Quark-Gluon Plasma:
$1.7 \times 10^{12}$ °C ≈ 150 MeV

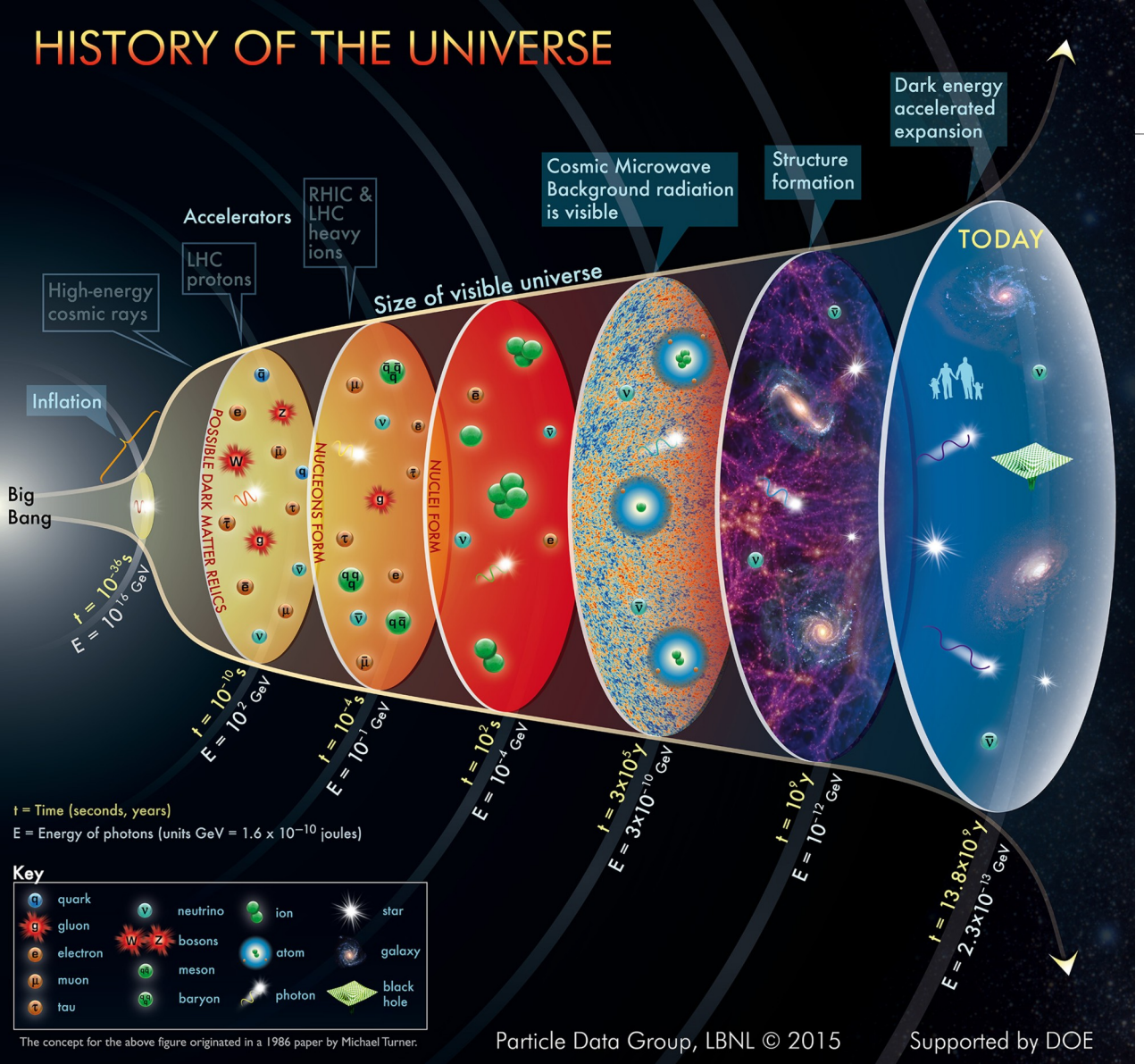


# Quark-gluon plasma

- Existed in the early universe
- Produced in heavy ion collisions

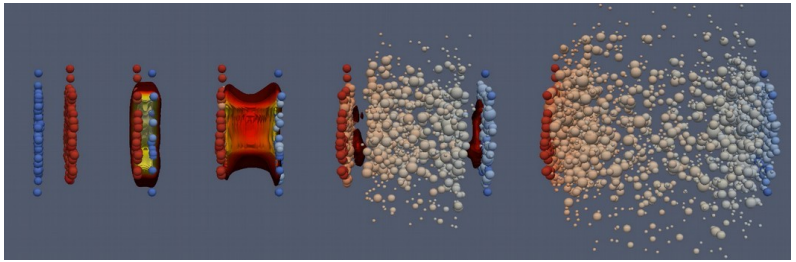

# Stages of a heavy-ion collision

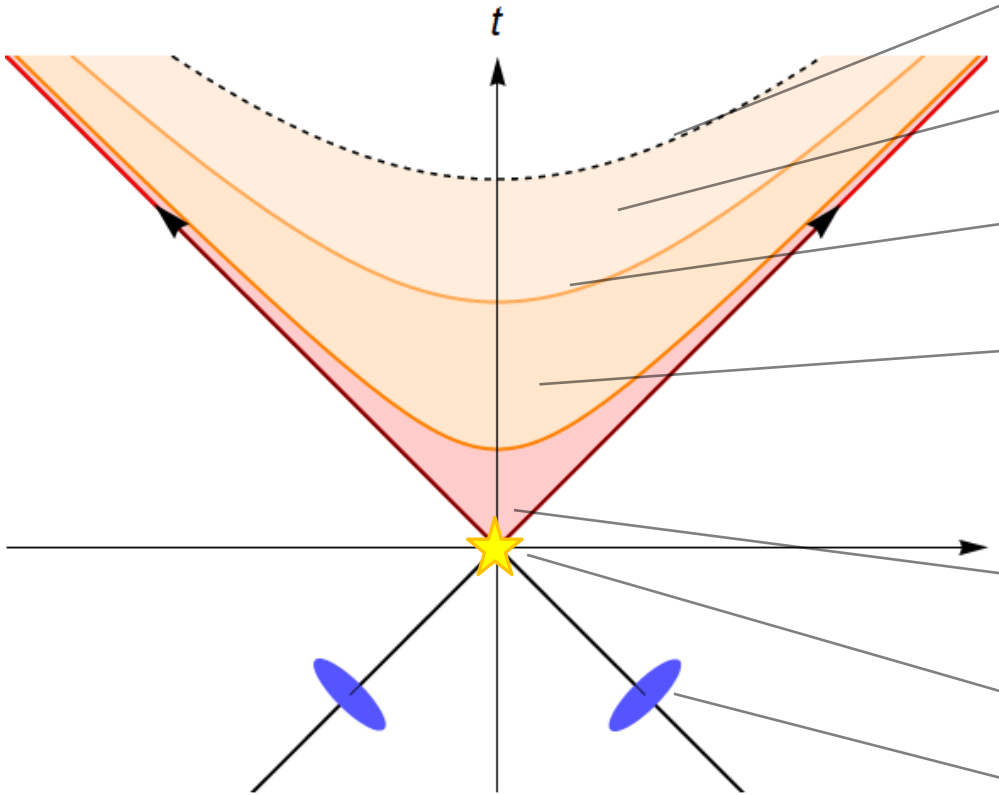


**Freeze-out** (τ ≈ 15 fm/*c*):
interactions stop

**Hadronic gas** (τ ≈ 10 - 15 fm/*c*)**:** hadrons
(kinetic transport theory)

**Hadronization** (τ ≈ 10 fm/*c*)**:**
confinement transition → hadron formation

**QGP** (τ ≈ 1 - 10 fm/*c*)**:** quarks and gluons
(relativistic viscous hydrodynamics)

**Glasma** (τ ≈ 0 - 1 fm/*c*)**:** quasi-classical fields
(classical field equations)

**Collision event**

**Initial state:** Lorentz-contracted nuclei
(color glass condensate)

$$1\,\mathrm{fm}/c \approx 3.3 \cdot 10^{-24}\,\mathrm{s} \approx 3.3\,\mathrm{ys}$$

# Colored particle-in-cell method

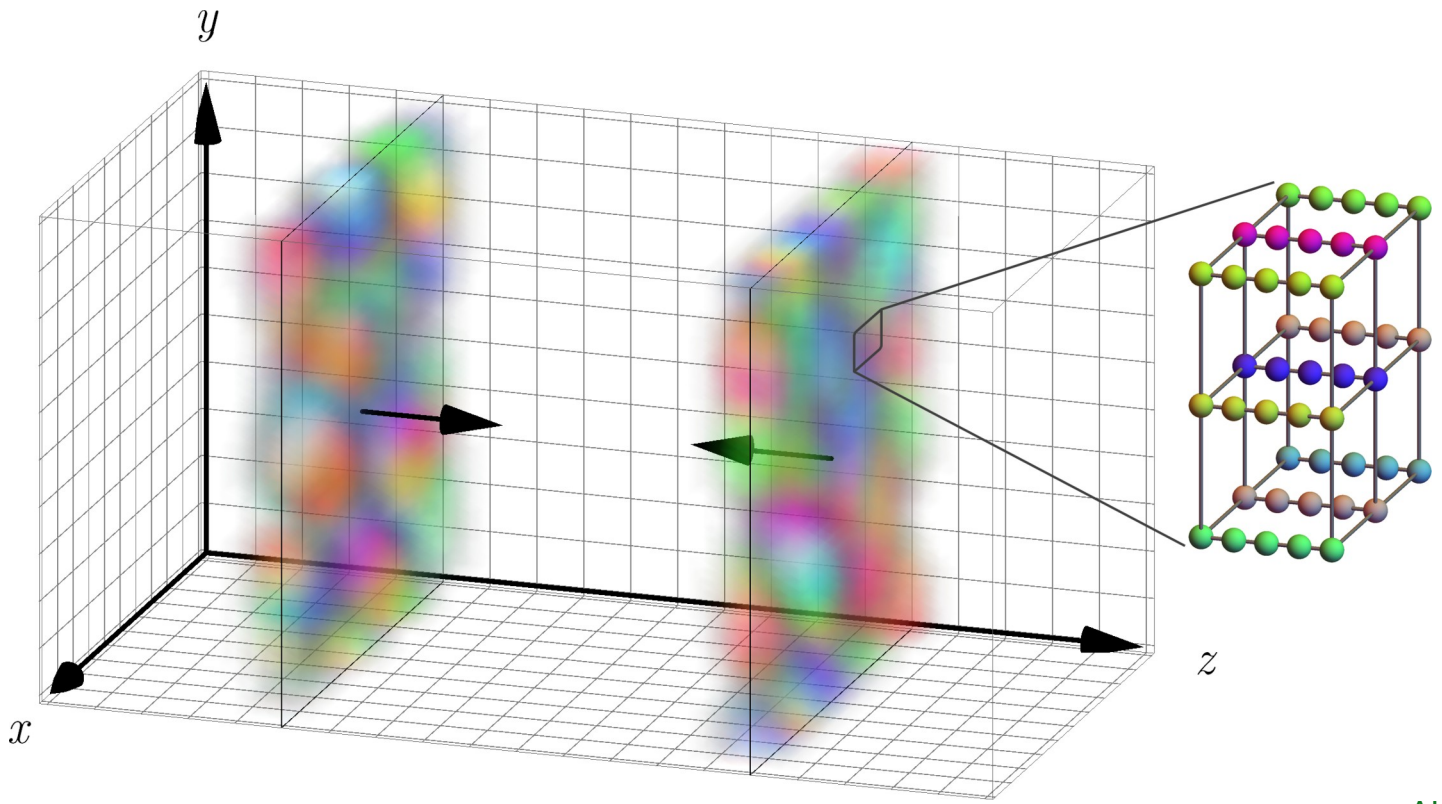


Generalization of the particle-in-cell method from plasma physics for strong interactions.

[A. Dumitru, Y. Nara, M. Strickland: PRD75:025016 (2007)]

Based on real-time lattice gauge theory in a classical regime.

AI, D. Müller, Phys. Lett. B 771 (2017) 74

# Dispersion-free propagation

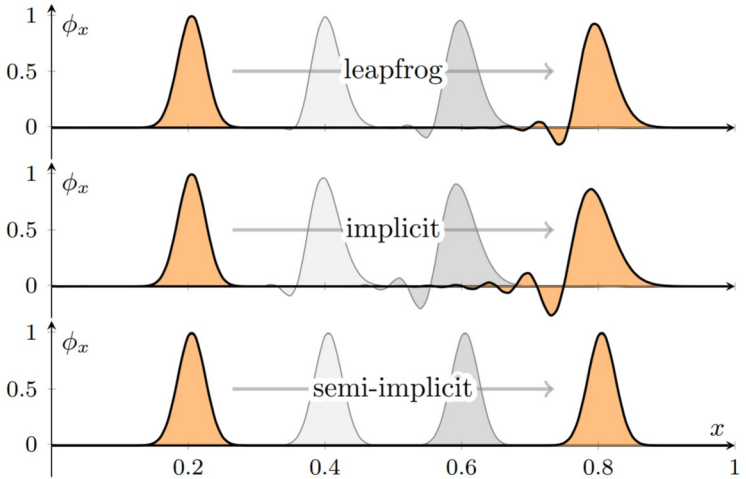


Standard **Wilson action**:

$$S[U] = \frac{V}{g^2} \sum_x \left( \sum_i \frac{1}{(a^0 a^i)^2} \operatorname{tr}\left(2 - U_{x,0i} - U^\dagger_{x,0i}\right) - \frac{1}{2} \sum_{i,j} \frac{1}{(a^i a^j)^2} \operatorname{tr}\left(2 - U_{x,ij} - U^\dagger_{x,ij}\right) \right)$$

**Variational integrator**: Discretized equations of motion from discretized action

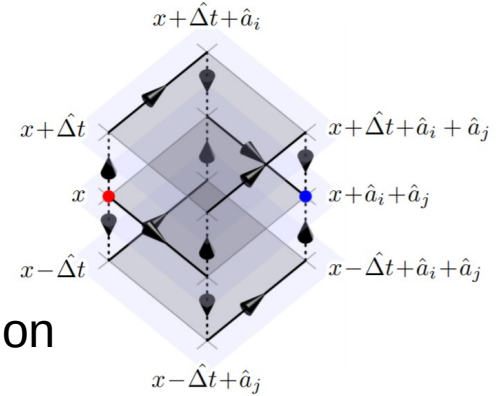


Discretized action for the **semi-implicit scheme**:

$$S[U] = \frac{V}{g^2} \sum_x \left( \frac{1}{(a^0 a^1)^2} \operatorname{tr}\left(C_{x,01} C^\dagger_{x,01}\right) + \sum_i \frac{1}{(a^0 a^i)^2} \operatorname{tr}\left(C_{x,0i} C^\dagger_{x,0i}\right) - \frac{1}{4} \sum_{i,|j|} \frac{1}{(a^i a^j)^2} \operatorname{tr}\left(C_{x,ij} M^\dagger_{x,ij}\right) - \frac{1}{4} \sum_{|j|} \frac{1}{(a^1 a^j)^2} \operatorname{tr}\left(C_{x,1j} W^\dagger_{x,1j} + \text{h.c.}\right) \right)$$

implicit part

semi-implicit part

with $C_{x,\mu\nu} \equiv U_{x,\mu} U_{x+\mu,\nu} - U_{x,\nu} U_{x+\nu,\mu}$

For details see:
AI, D. Müller, Eur.Phys.J. C78 (2018) no.11, 884

# Simulations of the collision process

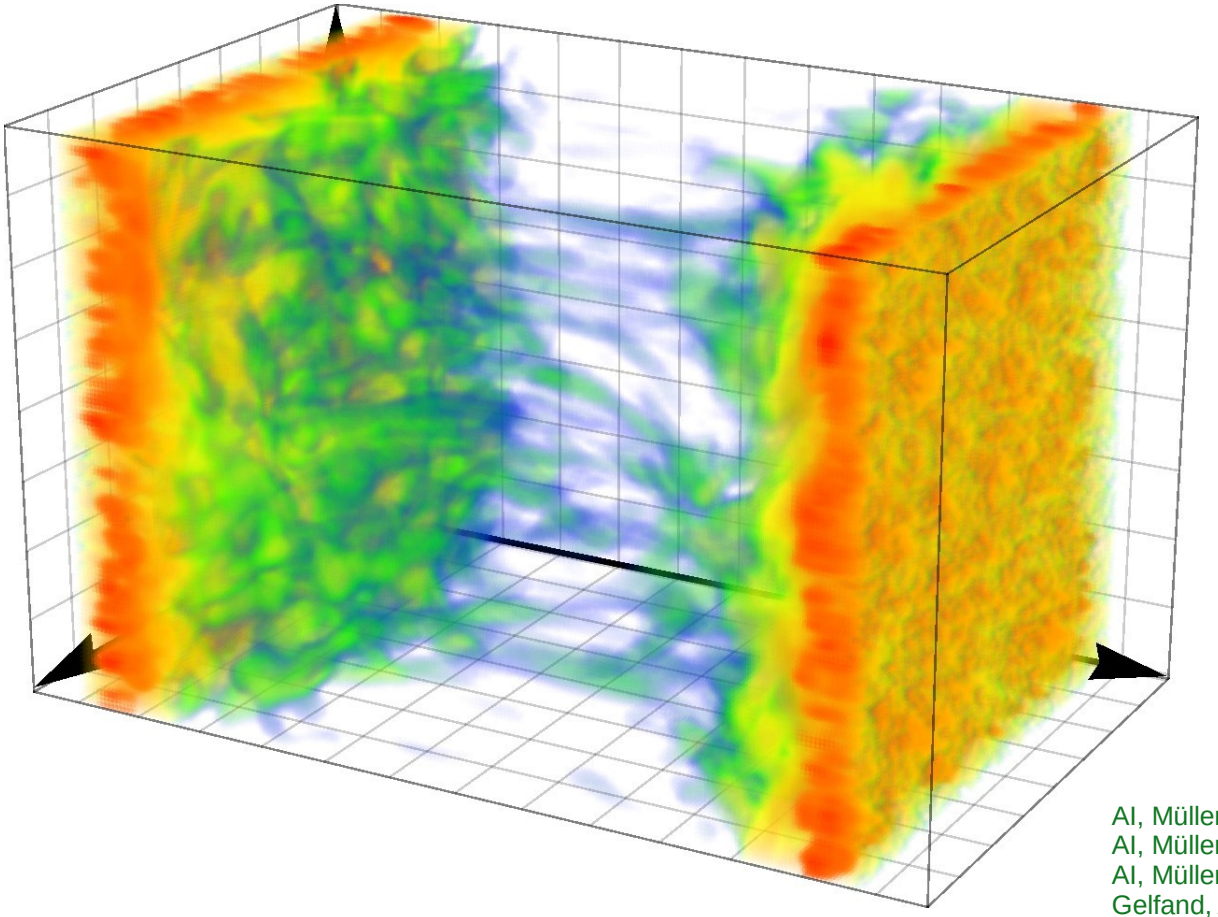

AI, Müller, Eur.Phys.J.A 56 (2020) 9, 243
AI, Müller, Eur.Phys.J. C78 (2018) no.11, 884
AI, Müller, Phys. Lett. B 771 (2017) 74
Gelfand, AI, Müller, Phys. Rev. D94 (2016) no.1, 014020

# Computational challenges

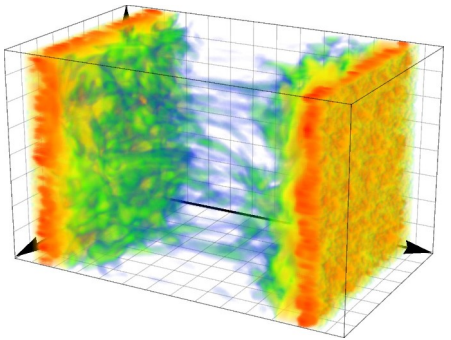

Simulating small part of nuclei
at RHIC energies:

γ-factor: 100
Lattice: 2048 × $192^2$ cells
Gauge group: SU(2)
Color sheets: 1
Simulation box: $(6\ \mathrm{fm})^3$

→ **25 GB** simulation data
→ **192 core hours** on
Vienna Scientific Cluster (VSC-3)

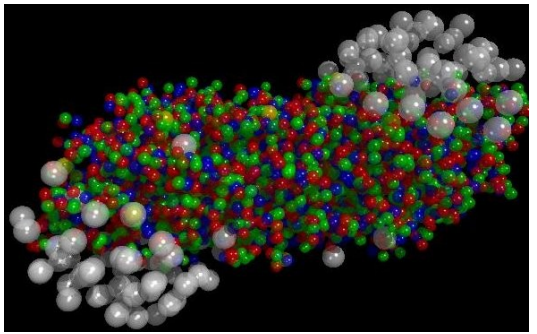

Simulating realistic off-central full size nuclei
at LHC energies:

γ-factor: 2500
Lattice: (25×20480) × $1920^2$ cells
Gauge group: SU(3)
Color sheets: 100
Simulation box: $(60\ \mathrm{fm})^3$

→ **25 PB** simulation data
→ **5 million core years** on VSC-3
(2020: 150 years on VSC-3; but only 130 TB RAM available)
(2023: 55 years on VSC-5; 355 TB RAM available)

# Convolutional neural networks

Dense neural network:

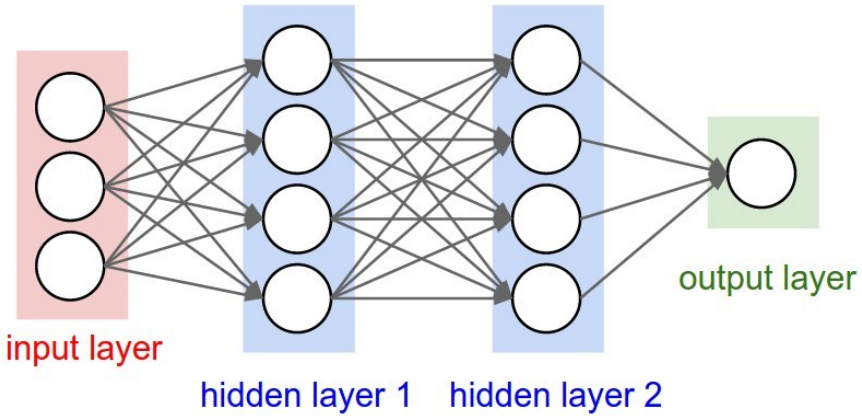


Image: https://cs231n.github.io/neural-networks-1/

→ Every input node connected to every output node

Convolutional Neural Network (CNN):

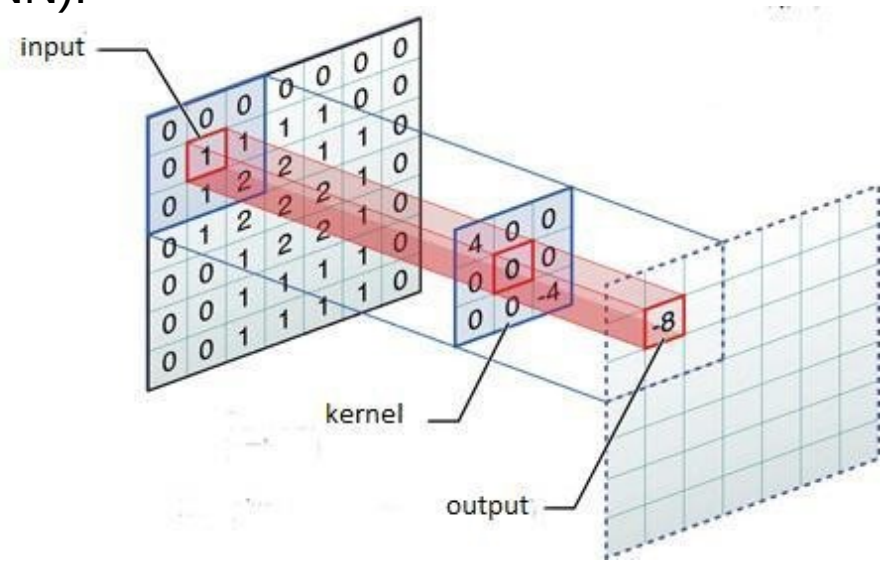


Image: https://towardsdatascience.com/convolutional-neural-networks-from-the-ground-up-c67bb41454e1

→ local information: only nodes „nearby“ are connected
→ Weight sharing by sliding the same kernel across the whole image

# Deep learning

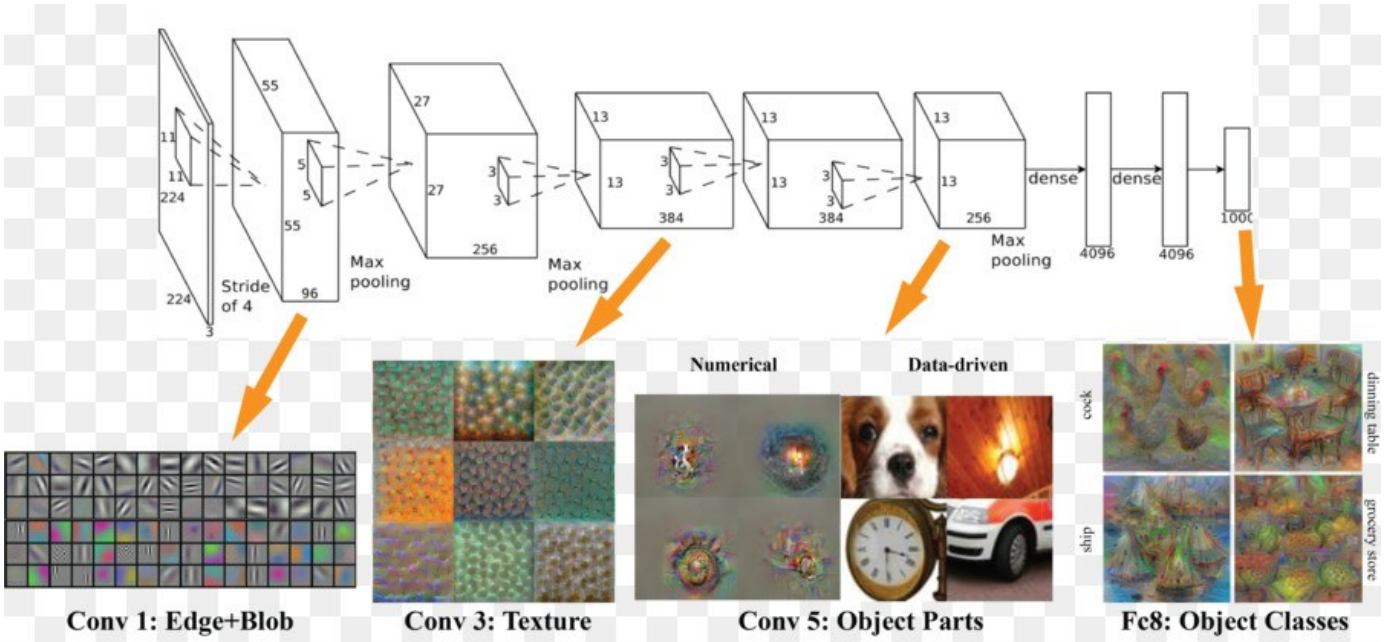


1960s: shallow neural networks
1960-70s: backpropagation
1980s: convolutional networks (CNN)

1990s: supervised deep learning
2006s: modern deep learning
2012: AlexNet (first GPU CNN)

# Equivariance (covariance) vs. invariance

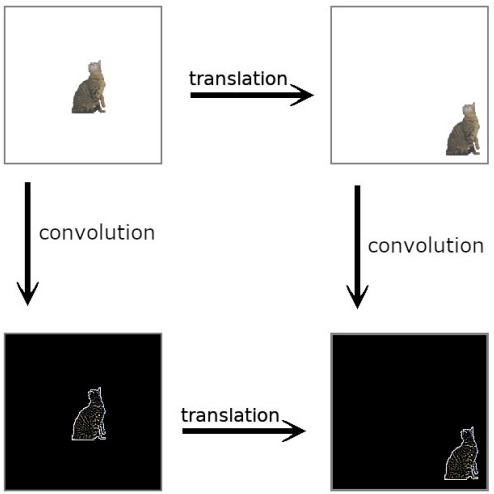


Equivariance

$$\Phi(L_g\, x) = L'_g\, \Phi(x)$$

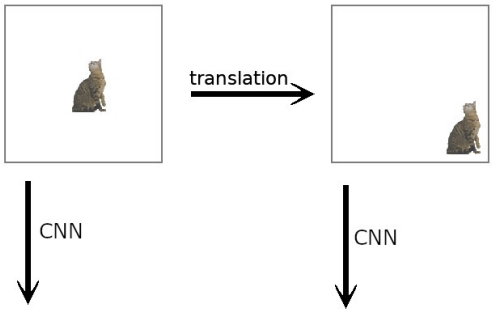


"cat" = "cat"

Invariance

$$\Phi(L_g\, x) = \Phi(x)$$

Adapted from: https://towardsdatascience.com/sesn-cec766026179

# Translational symmetry

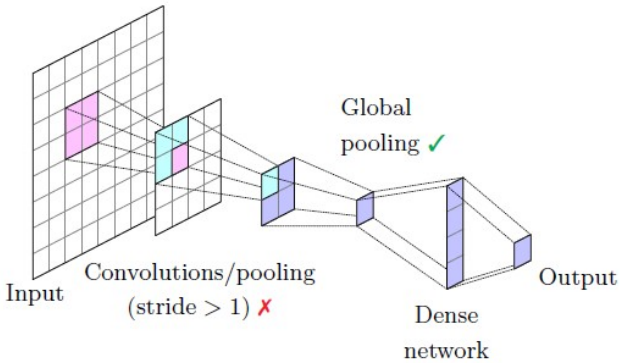


(b)Strided architecture (ST)

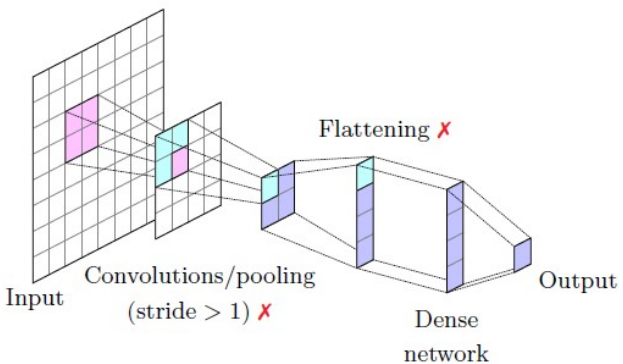


(c)Flattening architecture (FL)

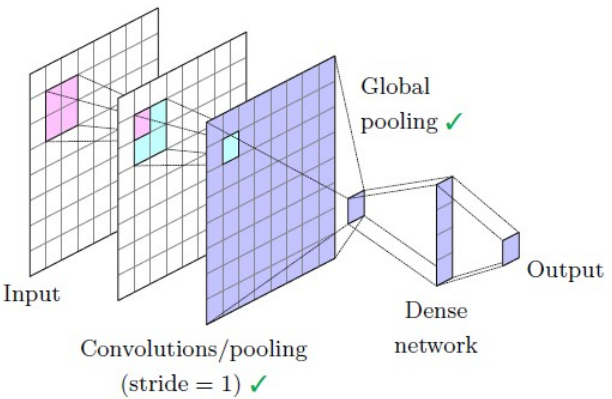


(a)Equivariant architecture (EQ)

Test regression tasks on observables of a scalar field model in 2 dimensions:

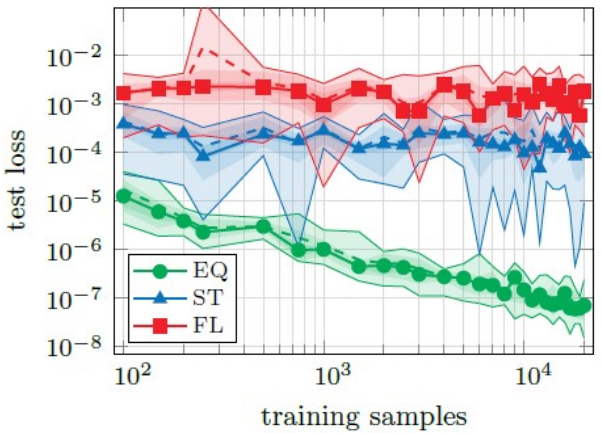


Bulusu, Favoni, AI, Müller, Schuh, Phys. Rev. D 104 (2021) 074504

# Symmetries on the lattice

Translational symmetry
→ Convolutional neural networks (CNNs)

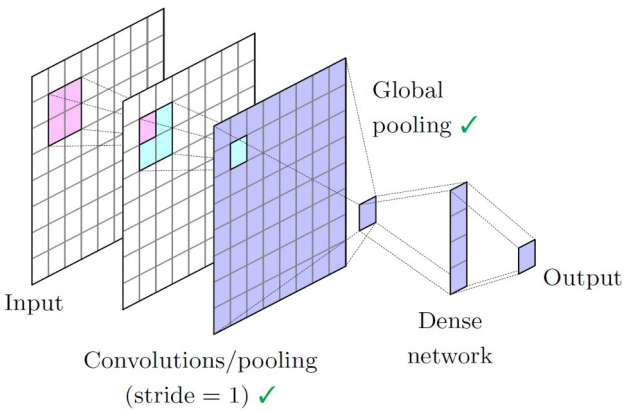


Bulusu, Favoni, AI, Müller, Schuh,
Phys. Rev. D 104 (2021) 074504

Rotation, mirror symmetry
→ Group equivariant CNNs (G-CNNs)

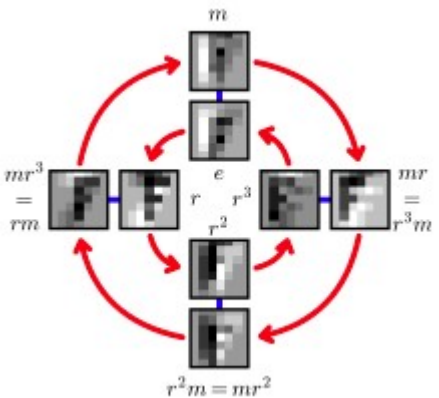


Cohen, Welling, ICML 2016

(see also talk by Daniel Schuh)

Lattice gauge symmetry
→ Lattice gauge equivariant CNNs (L-CNNs)

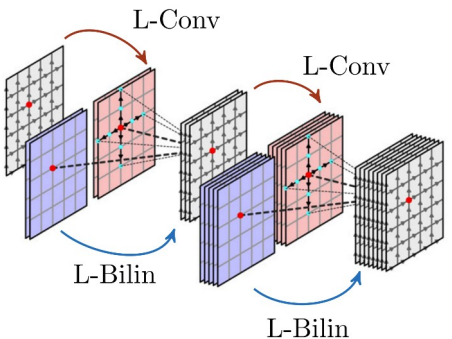


Favoni, AI, Müller, Schuh,
Phys.Rev.Lett. 128 (2022) 032003

# Wilson loops

## Wilson action

$$S_W[U] = \frac{2}{g^2} \sum_{x \in \Lambda} \sum_{\mu < \nu} \mathrm{Tr}\left[\mathbb{1} - U_{x,\mu\nu}\right]$$

## Plaquette

$$U_{x,\mu\nu} = U_{x,\mu} U_{x+\mu,\nu} U^{\dagger}_{x+\nu,\mu} U^{\dagger}_{x,\nu} =$$

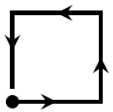

## Symanzik improved clover action

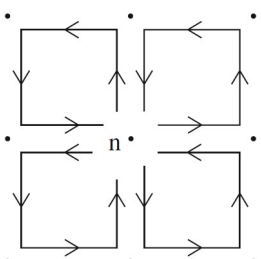


from: Gattringer, Lang (2010)

## Potential of static quark pair

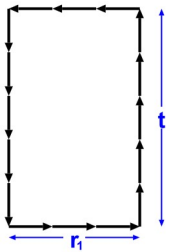


from: Bali, Phys.Rept. 343:1 (2001)

## Improved topological charge

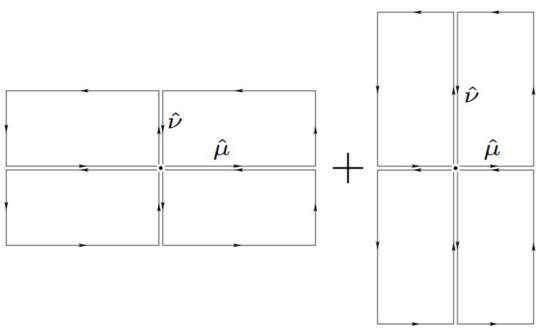


from: Alexandrou et al., Eur.Phys.J.C 80 (2020) 5, 424

## Improved real-time lattice actions

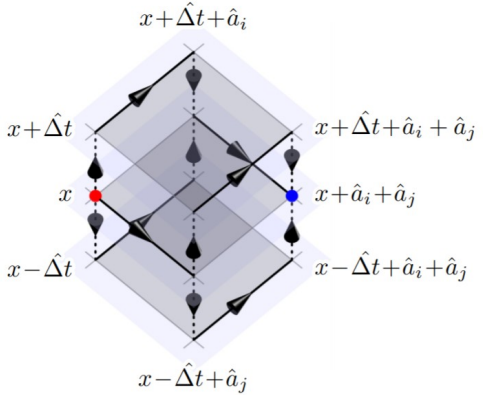


AI, Müller, Eur.Phys.J. C78 (2018) no.11, 884

# L-CNN data

Combine lattice links *U*
and locally transforming objects *W*

$$\text{tuple } (\mathcal{U}, \mathcal{W})$$

$$\mathcal{U} = \{U_{x,\mu}\} \text{ SU}(N_c) \text{ matrices}$$

$$\mathcal{W} = \{W_{x,i}\} \text{ with } W_{x,i} \in \mathbb{C}^{N_c \times N_c}$$

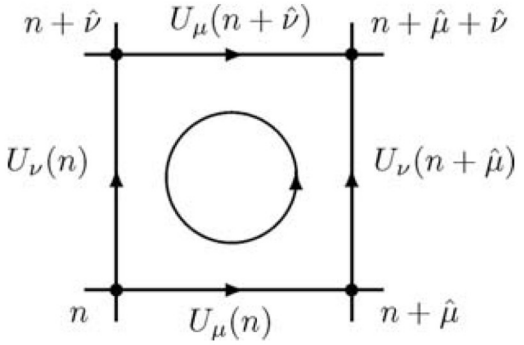


from: Gattringer, Lang (2010)

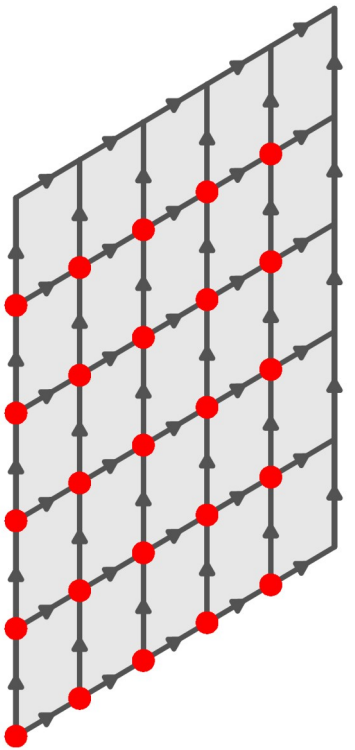

$$\mathcal{U} = \{U_{\mathbf{x},\mu}\}$$

$$\mathcal{W} = \{W_{\mathbf{x},\mu\nu}\}$$

Gauge transformation

$$T_\Omega U_{x,\mu} = \Omega_x U_{x,\mu} \Omega^\dagger_{x+\mu}$$

$$T_\Omega W_{x,i} = \Omega_x W_{x,i} \Omega^\dagger_x$$

Gauge equivariant (gauge covariant) function

$$f(T_\Omega \mathcal{U}, T_\Omega \mathcal{W}) = T'_\Omega f(\mathcal{U}, \mathcal{W})$$

Gauge invariant function

$$f(T_\Omega \mathcal{U}, T_\Omega \mathcal{W}) = f(\mathcal{U}, \mathcal{W})$$

# Lattice gauge equivariant layers

Convolution (L-Conv)

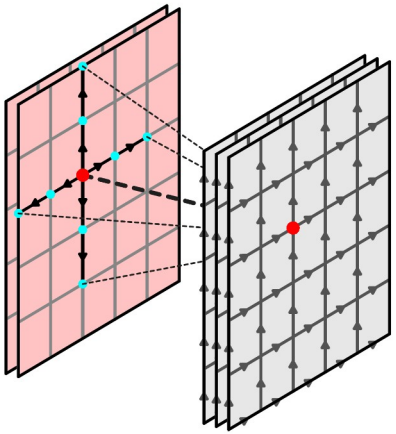

Convolution wish shared weights and proper parallel transport along coordinate axes

$$(\mathcal{U},\mathcal{W}) \to (\mathcal{U},\mathcal{W}')$$

$$W'_{\mathbf{x},i} = \sum_{j,\mu,k} \omega_{i,j,\mu,k} U_{\mathbf{x},k\cdot\mu} W_{\mathbf{x}+k\cdot\mu,j} U^{\dagger}_{\mathbf{x},k\cdot\mu}$$

Bilinear layer (L-Bilin)

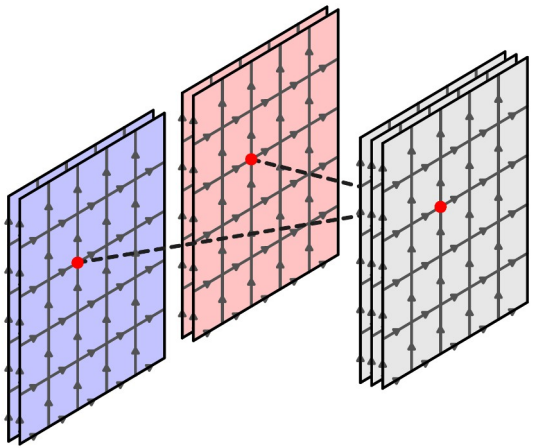

Multiply *W* at each lattice point

$$(\mathcal{U},\mathcal{W}) \times (\mathcal{U},\mathcal{W}') \to (\mathcal{U},\mathcal{W}'')$$

$$W''_{\mathbf{x},i} = \sum_{j,k} \alpha_{ijk} W_{\mathbf{x},j} W'_{\mathbf{x},k}$$

Trace layer

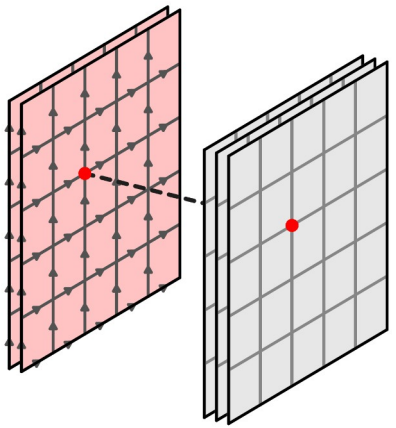

Generate gauge invariant output

$$w_{\mathbf{x},i} = \operatorname{Tr} W_{\mathbf{x},i} \in \mathbb{C}$$

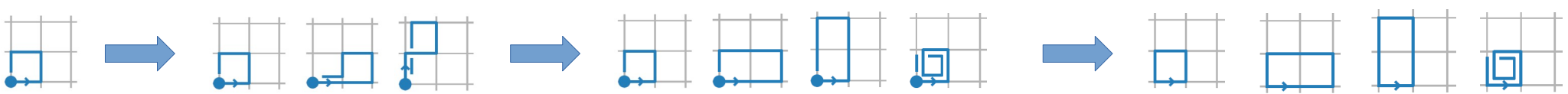

# Generic L-CNN

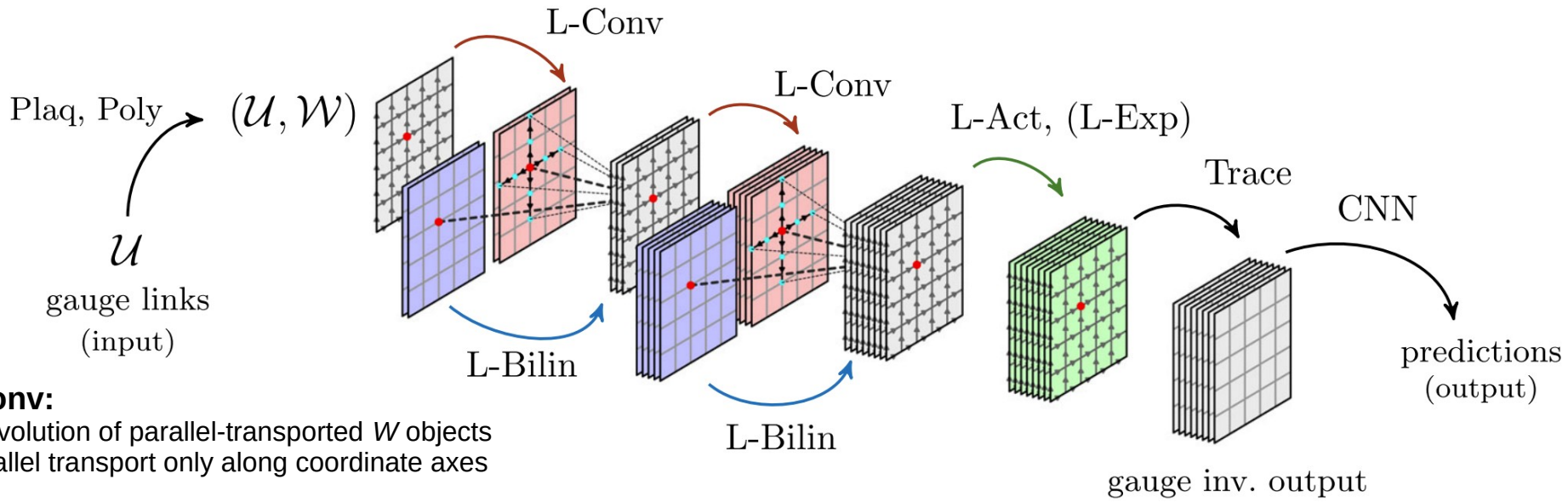


**L-Conv:**
* convolution of parallel-transported *W* objects
* parallel transport only along coordinate axes

**L-Bilin:**
* bilinear layer, product of locally transforming objects

**L-Act:**
* activation functions multiply *W* objects by scalar, gauge-invariant functions

**L-Exp:**
* update link variables using exponential map

**Trace:**
* calculate gauge invariant trace

**Plaq:**
* generate all possible plaquettes

**Poly:**
* generate all possible Polyakov loops

Favoni, AI, Müller, Schuh,
Phys.Rev.Lett. 128 (2022) 032003

# L-CNNs generate Wilson loops

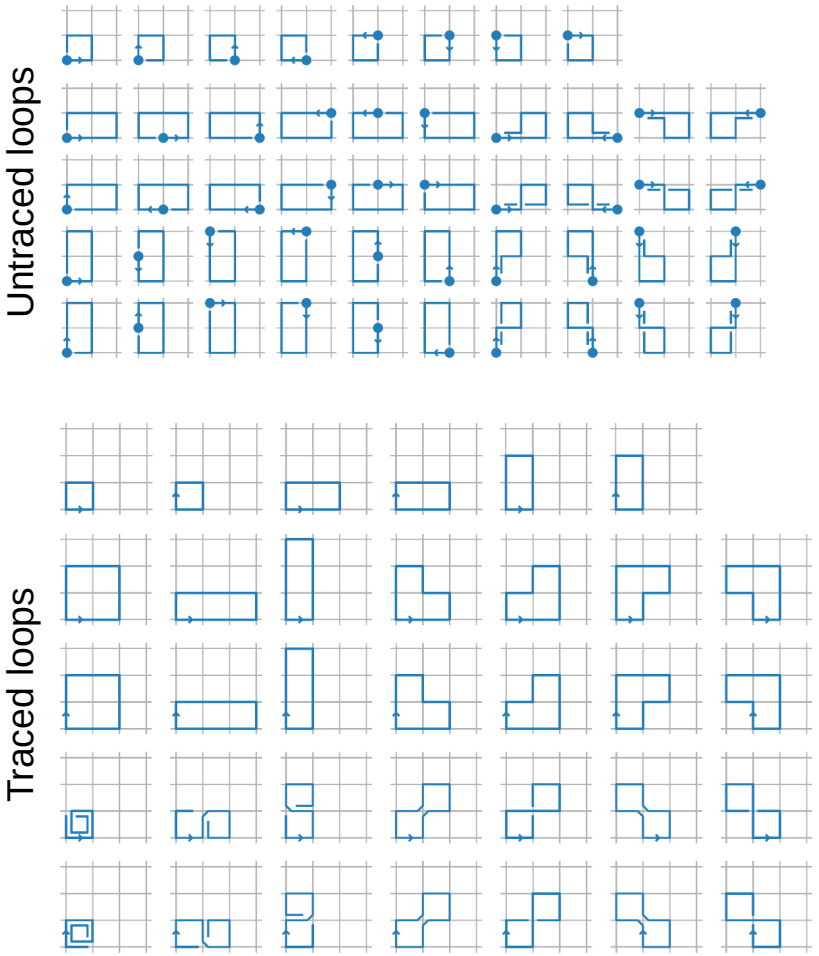


Number of traced Wilson loops covered by L-CNN architectures of various sizes in 1+1 D

| Length | Max | $W^{(1\times1)}$ | $W^{(1\times2)}$ | | | $W^{(2\times2)}$ | | |
|---|---|---|---|---|---|---|---|---|
| | | S | S | M | L | S | M | L |
| 0 | 1 | 1 | 1 | 1 | 1 | 1 | 1 | 1 |
| 2 | 0 | 0 | 0 | 0 | 0 | 0 | 0 | 0 |
| 4 | 2 | 2 | 2 | 2 | 2 | 2 | 2 | 2 |
| 6 | 4 | | 4 | 4 | 4 | 4 | 4 | 4 |
| 8 | 28 | | 4 | 4 | 4 | 22 | 22 | 22 |
| 10 | 152 | | | 8 | 8 | 48 | 76 | 76 |
| 12 | 1,010 | | | | 8 | 92 | 204 | 220 |
| 14 | 6,772 | | | | | 120 | 412 | 532 |
| 16 | 47,646 | | | | | 100 | 712 | 1,080 |
| 18 | 343,168 | | | | | 136 | 928 | 1,896 |
| 20 | 2,529,890 | | | | | 32 | 1,056 | 2,620 |
| 22 | 18,982,172 | | | | | 64 | 768 | 3,152 |
| $\geq$24 | | | | | | | 800 | 7,210 |
| Total | | 3 | 11 | 19 | 27 | 621 | 4,985 | 16,725 |
| Max.Len | | 4 | 8 | 10 | 12 | 22 | 28 | 34 |

Architectures differ in number of layers, kernel size, and number of channels.

Favoni, AI, Müller, Schuh, Phys.Rev.Lett. 128 (2022) 032003

# Sketch of proof for arbitrary Wilson loops

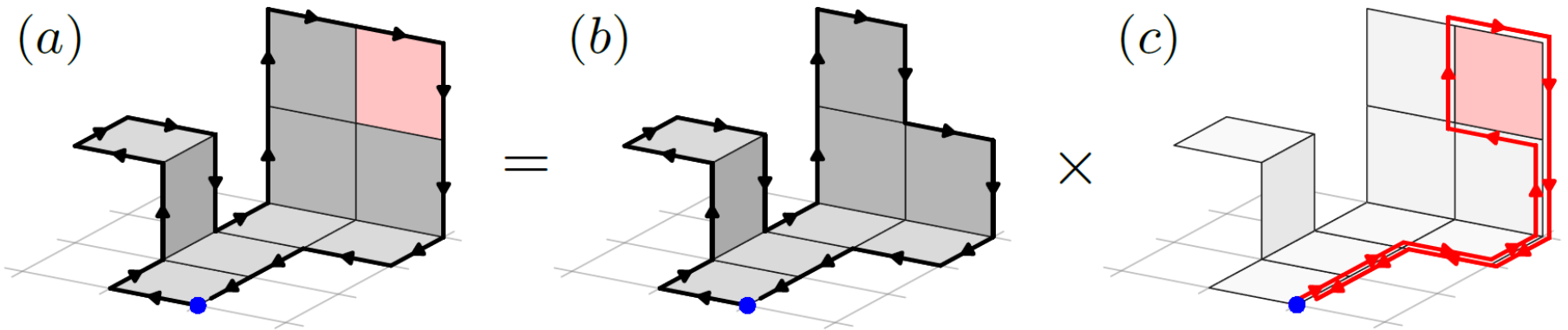


Favoni, AI, Müller, Schuh, Phys.Rev.Lett. 128 (2022) 032003

(a) An arbitrary contractible Wilson loop of *n* tiles ...
(b) … is composed (L-Bilin) of a Wilson loop of (*n*-1) tiles …
(c) … and a parallel-transported (L-Conv) plaquette (Plaq).

Non-contractible loops (like Polyakov loops) have to be added (Poly).

# Numerical results

1+1D

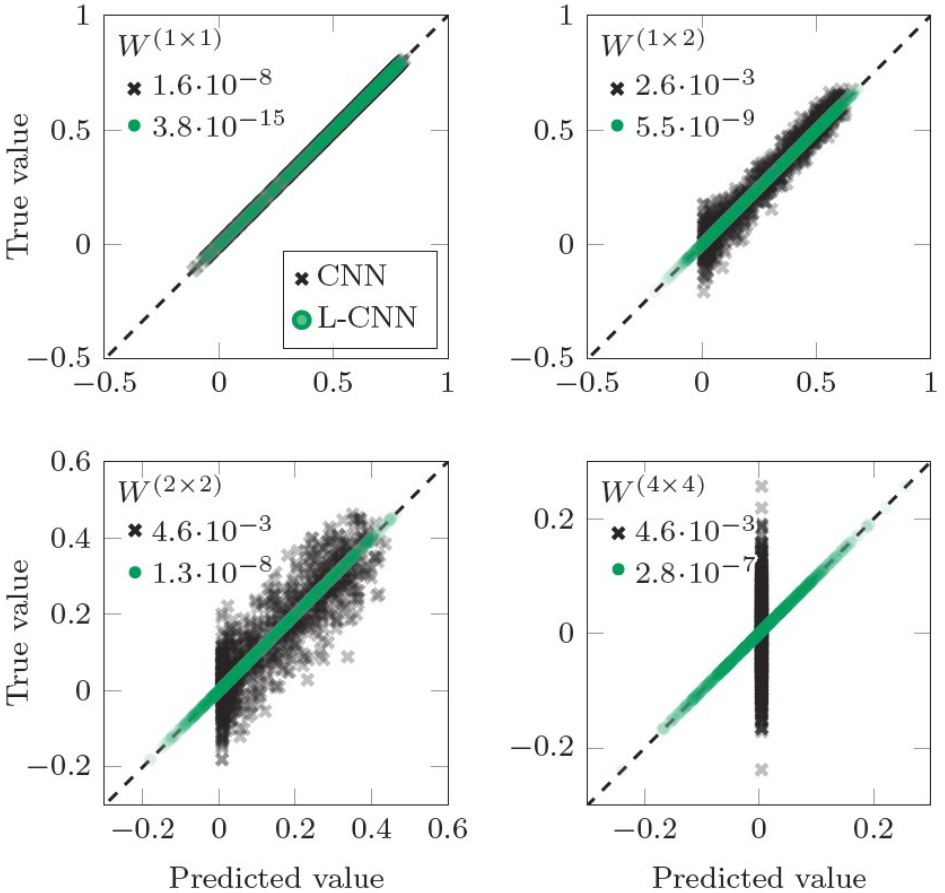


Regression task to learn value of rectangular Wilson loops:

$$W^{(m\times n)}_{x,\mu\nu} = \mathrm{Re}\,\mathrm{Tr}\left[U^{(m\times n)}_{x,\mu\nu}\right]$$

Lattice gauge equivariant CNN (L-CNNs, green) can learn the relation, while traditional convolutional neural networks (CNNs, black) struggle to find the solution.

Training on 8 × 8, testing from 8 × 8 up to 64 × 64

Compared best from:
100 L-CNN models (10 – $10^4$ trainable parameters, up to 4 L-Conv+L-Bilin)

2840 CNN models (100 – $10^5$ trainable parameters up to 6 layers, 512 channels, 4 activation functions)

Favoni, AI, Müller, Schuh, Phys.Rev.Lett. 128 (2022) 032003

# Analysis in terms of diagrams for 2D SU(2)

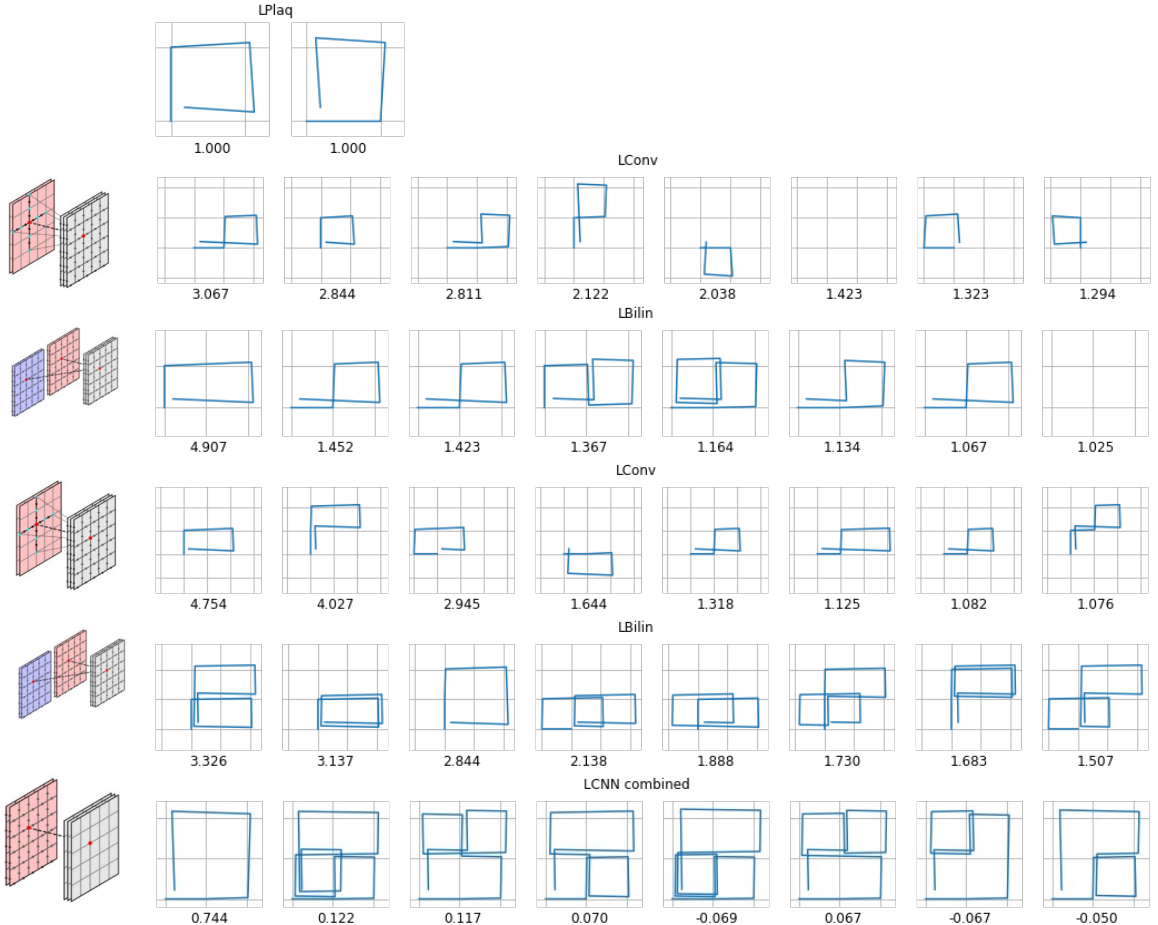


L-Plaq: 2 loops

L-Conv: 11 loops

L-Bilin: 144 loops

L-Conv: 721 loops

L-Bilin: 521284 loops

Trace: 21720 traced loops

# Train for different loop sizes

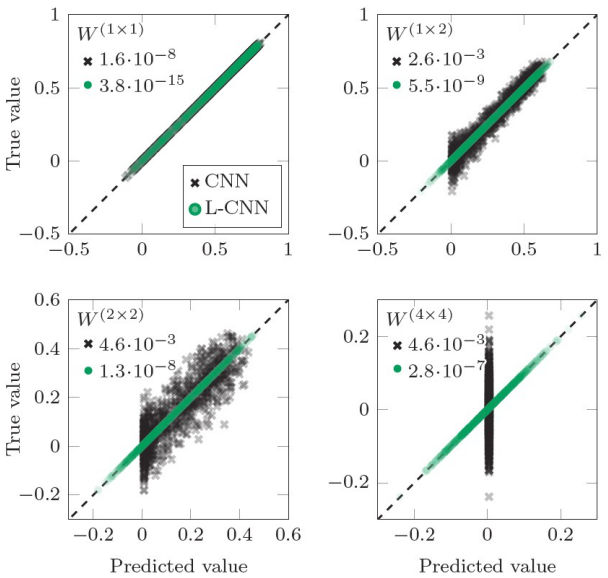


## 1x1 Plaquette

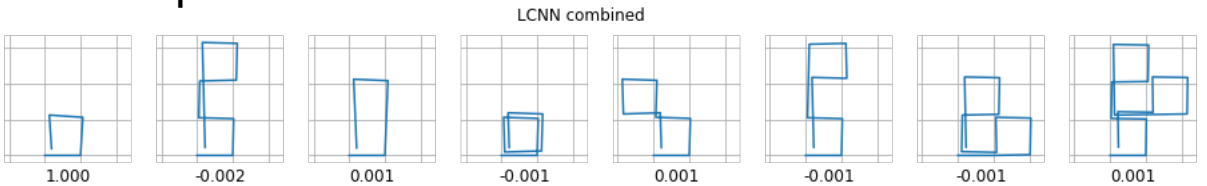


## 1x2 Wilson loop

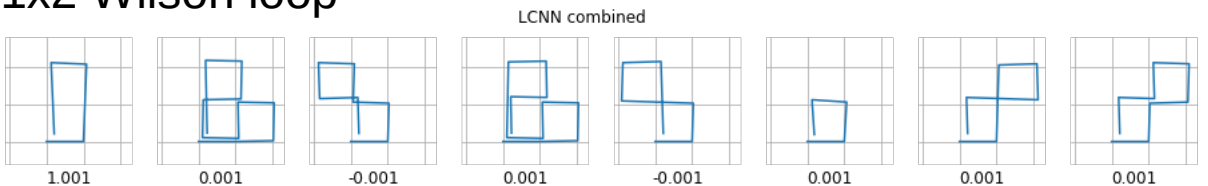


## 2x2 Wilson loop

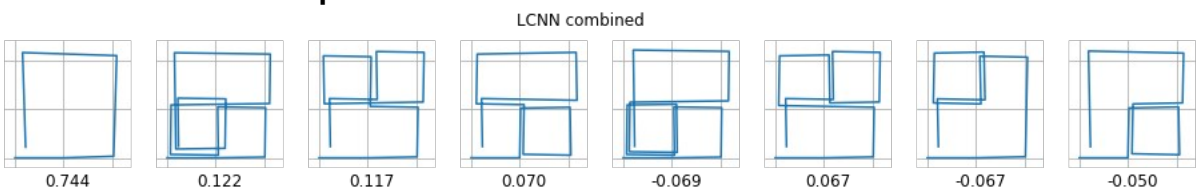

# Constraints for relating diagrams?

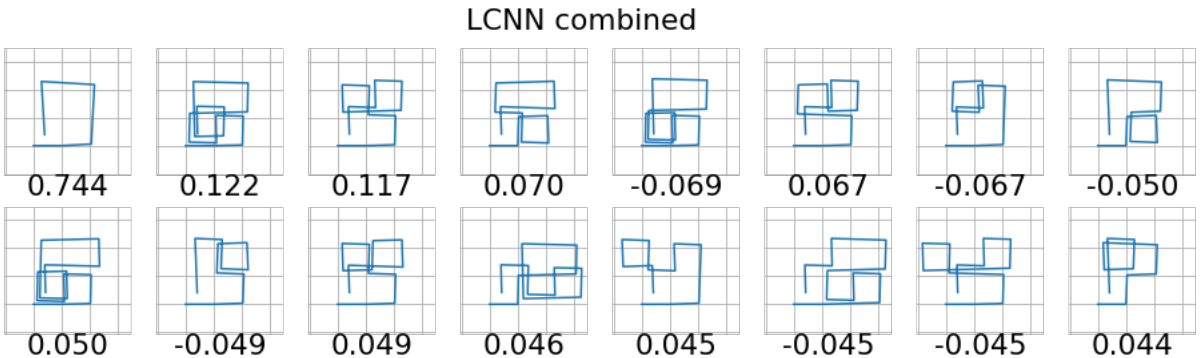


For SU(3): $$W^2 = \mathrm{tr}(W)W + \mathrm{tr}(W)^* \mathbb{1} + W^\dagger$$

For SU(2): $$W^2 = 2\,\mathrm{tr}(W)W - \mathbb{1}$$

Mandelstam contraints from the Cayley-Hamilton theorem
see e.g. Bacchio, Kessel, Schaefer, Vaitl, arXiv:2212.08469

# Another SU(2) relation

A general SU(2) matrix can be represented with real coefficients and Pauli matrices as:

$$A = a_0 \mathbb{1} + i a_1 \sigma_1 + i a_2 \sigma_2 + i a_3 \sigma_3$$

One can find the following relation:

$$\mathrm{tr}(ABC) - \mathrm{tr}(ACB) = \begin{vmatrix} a_1 & b_1 & c_1 \\ a_2 & b_2 & c_2 \\ a_3 & b_3 & c_3 \end{vmatrix}$$

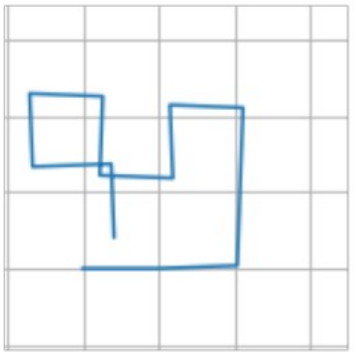


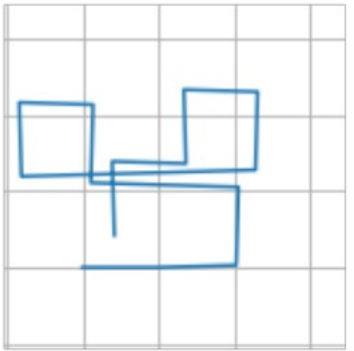


In particular:

$$\begin{aligned} \mathrm{tr}(ABC) - \mathrm{tr}(ACB) &= -\mathrm{tr}(AB^\dagger C) + \mathrm{tr}(ACB^\dagger) \\ &= -\mathrm{tr}(ABC^\dagger) + \mathrm{tr}(AC^\dagger B) \\ &= \mathrm{tr}(AB^\dagger C^\dagger) - \mathrm{tr}(AC^\dagger B^\dagger) \end{aligned}$$

# Missing contributions

Looking through all 21720 traced loops, indeed one can find the corresponding diagrams and extract their coefficients:

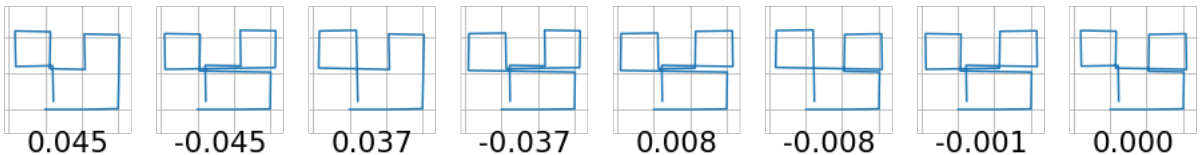


Contributions can be reshuffled:

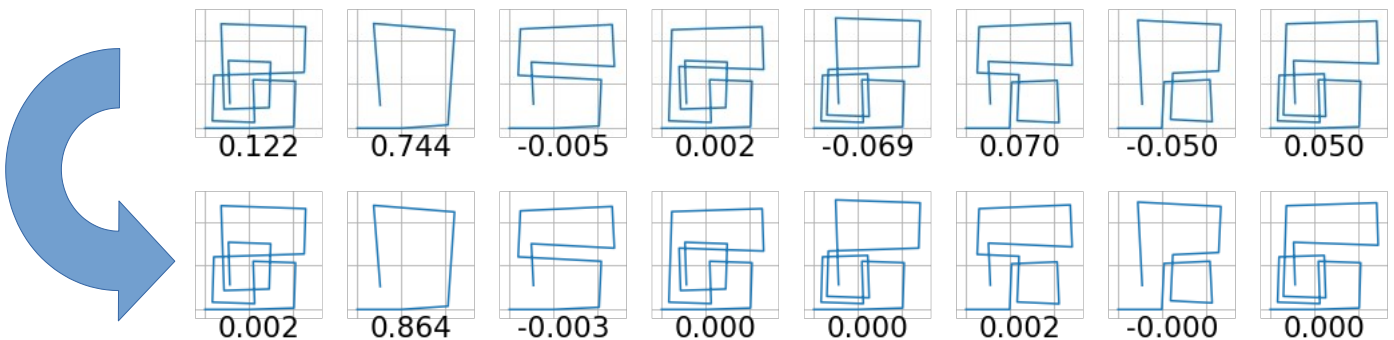


$$
\begin{aligned}
&\mathrm{tr}(ABC) - \mathrm{tr}(ACB) \\
=\;& -\mathrm{tr}(AB^\dagger C) + \mathrm{tr}(ACB^\dagger) \\
=\;& -\mathrm{tr}(ABC^\dagger) + \mathrm{tr}(AC^\dagger B) \\
=\;& \mathrm{tr}(AB^\dagger C^\dagger) - \mathrm{tr}(AC^\dagger B^\dagger)
\end{aligned}
$$

# Summary

Glasma simulations

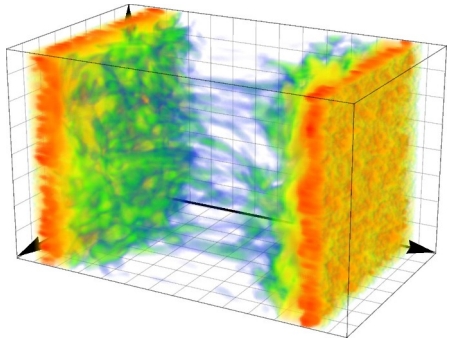

Ipp, Müller, Phys. Lett. B 771 (2017) 74
Gelfand, AI, Müller, Phys. Rev. D94 (2016) no.1, 014020

Translational equivariance

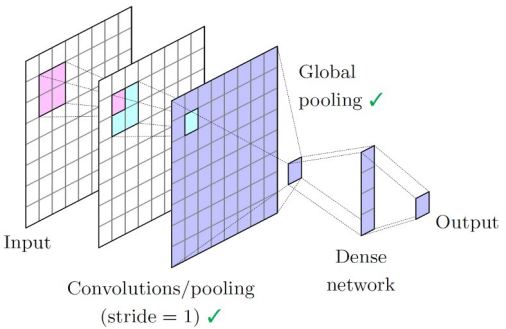


Bulusu, Favoni, AI, Müller, Schuh,
Phys. Rev. D 104 (2021) 074504

L-CNNs

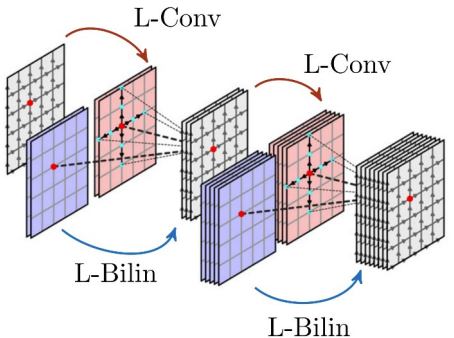


Favoni, AI, Müller, Schuh,
Phys.Rev.Lett. 128 (2022) 032003

Related talks:

- Daniel Schuh: robustness and geometric formulation of L-CNNs
- Matteo Favoni: neural ordinary differential equations
- Urs Wenger: fixed point action for coarse lattices
- Kieran Holland: learn the fixed point action with L-CNNs

David Müller

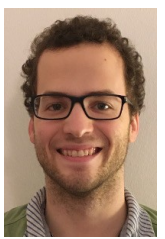

Daniel Schuh

Matteo Favoni

**Open source:** https://gitlab.com/openpixi/lge-cnn